

Cooling of Accelerated Nucleons and Neutrino Emission in Gamma-Ray Bursts

Katsuaki Asano

*Division of Theoretical Astronomy, National Astronomical Observatory of Japan, 2-21-1
Osawa Mitaka Tokyo, Japan*

asano@th.nao.ac.jp

ABSTRACT

Using Monte Carlo simulations, we demonstrate photopion production from Fermi-accelerated protons and the resulting neutrino production in gamma-ray bursts. Unless internal shocks occur at quite large distance from the center, ultra high-energy protons are depleted by photopion production and synchrotron radiation. Internal shocks at fiducial distance cause neutrino bursts, which accompany gamma-ray bursts originating from electromagnetic cascades.

Subject headings: gamma rays: bursts—cosmic rays—neutrinos

1. INTRODUCTION

The rapid time variabilities and the compactness problem (see, e.g., a review by Piran 1999) suggest that gamma-ray bursts (GRBs) should arise from internal shocks within relativistic flows. In the standard model a strong magnetic field is generated, and electrons are Fermi-accelerated in shocked regions. Because of the high Lorentz factor of the flows, synchrotron radiation by accelerated electrons is blue-shifted, and observed as gamma-ray photons.

The physical conditions in the shocked region imply (Waxman 1995) that protons may be also Fermi-accelerated to energies $> 10^{20}$ eV. If the total energy of protons, accelerated over the energy range 10^{19} - 10^{21} eV, is comparable to the energy of the gamma-rays, it can explain the flux of ultra-high-energy cosmic rays (UHECRs). This is an attractive idea for the cosmic-ray source.

High energy protons in the GRB photon field can create high-energy neutrinos via photopion production (Waxman and Bahcall 1997, 1999; Guetta et al. 2001; Dermer and

Atoyan 2003; Guetta et al. 2004). If the above prediction is true, a 1km^2 neutrino detector may detect neutrinos correlated with GRBs in the near future (Waxman and Bahcall 1997; Wick et al. 2004). However, if the proton photopion “optical depth” is much higher than unity, protons lose their energies in GRB sources. In this case GRBs cannot be the sources of UHECRs. Asano and Takahara (2003) (hereafter AT03) analytically show that high-energy protons cool rapidly via photopion production for fiducial parameters in GRB physics and that most of the proton energy converts to photons via π^0 decay, pion synchrotron, muon synchrotron, and the electromagnetic cascade of electron-positron pairs.

In this paper, using the Monte Carlo method, we simulate numerically the proton cooling and resulting neutrino emission in order to confirm quantitatively whether GRBs can be sources of UHECRs or not. Our method pursues energy loss processes of each nucleon interacting with photons and the magnetic field during the dynamical timescale. Therefore, we can treat energy loss processes correctly even in the case that a nucleon creates pions multiple times in the dynamical timescale. Dermer and Atoyan (2003) carried out similar calculations using a different method from ours. Our purpose is to obtain a physical condition to produce UHECRs, while Dermer and Atoyan (2003) mainly discussed neutrino production. In §2 we explain our model and method. The physical situation we consider is clearly shown. The numerical results are in §3. An analytically detailed description of the results can be found in AT03. Our conclusions are summarized in §4.

2. MODEL AND METHOD

We simulate nucleon cooling in the GRB photon field by the Monte Carlo method. We adopt a relatively low GRB energy and a small magnetic field for UHECR production to be as advantageous as possible. The situation we consider is as follows.

In the standard model gamma-ray photons are emitted from shocked shells moving with the bulk Lorentz factor $\Gamma > 100$ (see, e.g., a review by Piran 1999). In most cases the observed isotropic energies of GRBs are larger than 10^{52} ergs (Frail et al. 2001), and the number of pulses per burst is less than 10 (Mitrofanov et al. 1998). According to the above facts, we consider one shell of $\Gamma = 300$, in which gamma-ray photons are produced, and the total energy of those photons is $E_\gamma = 10^{51}$ ergs in spherical symmetry. The shell width is constrained by the observed variability time-scale, $\delta t > 1$ ms, and the duration time, ~ 10 s. Therefore, we assume that the shell width in the shell rest frame l is in the range of 10^{10} - 10^{14} cm. This implies the average luminosity $L = 9 \times 10^{49}$ - 9×10^{53} ergs s^{-1} . The photon energy density $U_\gamma = E_\gamma / (4\pi\Gamma R^2 l)$ in the shell rest frame depends on the radius $R \sim \Gamma^2 c \delta t$ where an internal shock occurs. In order to accelerate protons to energies $> 10^{20}$ eV, the internal

shocks should occur at radii $\geq 10^{13}$ cm (Waxman 1995). Therefore, we consider cases with $R \geq 10^{13}$ cm only. The energy density of magnetic field $U_B = B^2/8\pi$ is assumed to be $0.1U_\gamma$.

In our simulation, adopting the typical observed GRB spectra, the photon number density in the energy range $\epsilon_\gamma + d\epsilon_\gamma$ in the shell rest frame is set at $n(\epsilon_\gamma) \propto \epsilon_\gamma^{-1}$ for $1 \text{ eV} < \epsilon_\gamma < 1 \text{ keV}$ and $\epsilon_\gamma^{-2.2}$ for $1 \text{ keV} < \epsilon_\gamma < 10 \text{ MeV}$. The break energy 1 keV corresponds to 300 keV in the observer frame. For $\epsilon_\gamma < 1 \text{ eV}$ the synchrotron self absorption may be crucial (Granot et al. 2000), while the pair absorption may be crucial for $\epsilon_\gamma > 10 \text{ MeV}$ (e.g., see AT03). Thus, we neglect photons in such energy regions.

Since GRBs are possible sources of UHECRs with energies $> 10^{20} \text{ eV}$, we assume Fermi accelerated protons are injected in the energy range of $\epsilon_p = 10^{10}\text{-}10^{19} \text{ eV}$ in the shell rest frame as $\dot{N}(\epsilon_p) \propto \epsilon_p^{-2}$. Although the lowest energy of Fermi-accelerated particles is unknown, it is natural to consider that accelerated protons are distributed to quite a lower energy.

Relativistic protons ($\epsilon_p = \gamma_p m_p c^2 \gg m_p c^2$) in the GRB photon field create pions and lose their energies via photopion production. In the shell rest frame the photon distribution is isotropic. Then, the time scale of photopion production, t_π , is written as

$$t_\pi^{-1}(\gamma_p) = 2\pi c \int_{-1}^1 d\mu (1 - \beta_p \mu) \int d\epsilon_\gamma \frac{n(\epsilon_\gamma)}{4\pi} \sigma_\pi(\chi), \quad (1)$$

where $\beta_p = \sqrt{1 - 1/\gamma_p^2} \simeq 1$ and μ is the cosine of the photon incident angle. From Stecker (1968), based on experiments, we approximate the photopion production cross section by a broken power-law profile as $\sigma_\pi(\chi) = 5 \times 10^{-28} (\chi/590)^{3.2} \text{ cm}^2$ for $290 < \chi < 590$ and $\sigma_\pi(\chi) = 5 \times 10^{-28} (\chi/590)^{-0.7} \text{ cm}^2$ for $590 < \chi < 9800$, where $\chi m_e c^2$ is the photon energy in the proton rest frame. The energy of a photon is expressed as $\epsilon_\gamma = \chi m_e c^2 / \gamma_p (1 - \beta_p \mu)$.

Secondary neutrons produced in the channel with isospin flip, $p\gamma \rightarrow n\pi^+$, also create pions on almost the same time-scale as t_π . We use equation (1) for both protons and neutrons. In the Δ -approximation (Stecker 1973) the creation ratio $\pi^\pm : \pi^0$ is $1 : 2$. In the power-law target photon field, however, the ratio $\pi^\pm : \pi^0$ is close to $2 : 1$ (Rachen and Mészáros 1998), because the charged pion production rate increases away from the Δ -resonance. So, we adopt $\pi^\pm : \pi^0 = 2 : 1$ in this simulation. For simplicity the nucleon inelasticity is fixed as $K \equiv \Delta\epsilon_p/\epsilon_p = \Delta\epsilon_n/\epsilon_n = 0.2$, and the process of multiple pion production, which enhances the nucleon cooling efficiency, is neglected.

Extremely high energy protons can cool via synchrotron radiation with the power per unit photon energy

$$\frac{dW}{dt d\epsilon_\gamma} = \frac{\sqrt{3} e^3 B \sin \alpha}{h m_p c^2} F(x), \quad (2)$$

where $x = 2m_p c \epsilon_\gamma / (3\gamma_p^2 \hbar e B \sin \alpha)$ and $F(x)$ is the synchrotron function (Rybicki and Lightman 1979). The pitch angle α is determined from random numbers in our Monte Carlo simulation. The cooling time scale due to synchrotron radiation is $t_{\text{SY}} = 3(\gamma_p - 1)m_p^3 c^5 / 2e^4 B^2 \gamma_p^2 \beta_p^2 \sin^2 \alpha$.

Another possible mechanism of the proton cooling is inverse Compton (IC) scattering. The scattering rate is obtained from the Klein-Nishina cross section σ_{KN} (Rybicki and Lightman 1979) by exchanging mass $m_e \rightarrow m_p$. In the proton rest frame, when a photon with energy ϵ'_0 is scattered, the energy of the scattered photon is

$$\epsilon'_1 = \frac{\epsilon'_0}{1 + \frac{\epsilon'_0}{m_p c^2}(1 - \mu_s)}, \quad (3)$$

where μ_s is the cosine of the scattering angle. The probability distribution of the scattering angle is

$$P_\mu \propto \frac{\epsilon'_1}{\epsilon_0'^2} \left(\frac{\epsilon'_0}{\epsilon'_1} + \frac{\epsilon'_1}{\epsilon'_0} - (1 - \mu_s^2) \right). \quad (4)$$

The Lorentz transformation yields the scattered photon energy ϵ_1 in the shell rest frame. The cooling time-scale due to IC is

$$t_{\text{IC}}^{-1}(\gamma_p) = \frac{1}{(\gamma_p - 1)m_p c^2} 2\pi c \int_{-1}^1 d\mu (1 - \beta_p \mu) \int d\epsilon_\gamma (\epsilon_1 - \epsilon_\gamma) \frac{n(\epsilon_\gamma)}{4\pi} \sigma_{\text{KN}}(\epsilon'_0), \quad (5)$$

where $\epsilon'_0 = \gamma_p \epsilon_\gamma (1 - \beta_p \mu)$. To obtain t_{IC} , the numerical integration is carried out with μ_s determined from equation (4). This numerical integration process also gives the IC spectra at once.

We pursue 2.7×10^4 nucleons in each computation. Given a nucleon energy, the cooling time scales t_π , t_{SY} , and t_{IC} are determined. Let us denote the cooling time scale due to photon emission by t_γ , which satisfies $t_\gamma^{-1} = t_{\text{SY}}^{-1} + t_{\text{IC}}^{-1}$. Assuming that nucleons interact with photons and the magnetic field during the dynamical time scale $t_d = l/c$, we pursue the nucleon cooling process by a time step $\Delta t = \min(t_\pi, t_\gamma)/10$ and $t_\pi/10$ for protons and neutrons, respectively. The time step will change as nucleons lose their energies. The pion production probability in each time step is $1 - \exp(-\Delta t/t_\pi)$. If nucleons create charged pions, the species of the nucleons is changed ($p \leftrightarrow n$). After t_d s have passed, nucleons are considered to escape from the shell.

The neutron-decay emissions will produce nonthermal emission signatures. However, we can distinguish those emissions from the prompt burst, since the flux of neutrinos and photons originated from the neutron-decay is faint because of the long decay time-scale. We do not discuss those emissions below.

3. RESULTS

3.1. Proton cooling

The time-scales t_π , t_{SY} , and t_{IC} are proportional to $R^2 l$, while the dynamical time-scale $t_d \propto l$ (see AT03). The proton cooling process is determined by the ratios $\tau_\pi = t_d/t_\pi$, $\tau_{\text{SY}} = t_d/t_{\text{SY}}$, and $\tau_{\text{IC}} = t_d/t_{\text{IC}}$, which are proportional to R^{-2} . Thus, the proton cooling process is independent of l . Under the situation we consider, the proton cooling efficiency depends on the total photon energy E_γ and the radius R , rather than on the luminosity $L \propto E_\gamma/l$.

In Figure 1 we plot the ratios $\tau_\pi, \tau_{\text{SY}}, \tau_{\text{IC}}$ for $R = 10^{13}$ cm and $E_\gamma = 10^{51}$ erg. From the condition to create pions $\epsilon_p \epsilon_\gamma \geq 0.2 \text{ GeV}^2$, the behavior of τ_π is explained as follows. For $\Gamma \epsilon_p < 6 \times 10^{16}$ eV, protons produce pions with photons whose energies are above the break energy $\Gamma \epsilon_\gamma = 300$ keV [$n(\epsilon_\gamma) \propto \epsilon_\gamma^{-2.2}$]. In this case the number of the interacting photons is proportional to $\sim \epsilon_p^{1.2}$, which implies $\tau_\pi \propto \epsilon_p^{1.2}$. Above 6×10^{16} eV protons interact with photons in a low-energy region [$n(\epsilon_\gamma) \propto \epsilon_\gamma^{-1.0}$]. As a result, τ_π is nearly constant in this energy region. It is easily confirmed that the simple approximation in Waxman and Bahcall (1997), which was adopted in simulations in Guetta et al. (2001, 2004), produces a close value to our numerical estimate, τ_π . Since Waxman and Bahcall (1997) adopted a very low energy, $E_\gamma = L \delta t = 10^{48}$ ergs for a shell, the pion production efficiency in their case becomes lower than ours. Beyond 6×10^{19} eV, the threshold energy of target photons to create pions is below the cut-off energy (0.3 keV in the observer frame). As a result, τ_π decreases above this energy.

For $\Gamma \epsilon_p > 3 \times 10^{20}$ eV, the proton synchrotron cooling dominates photopion production. Although the photon energy density is larger than the magnetic energy density ($U_B = 0.1 U_\gamma$), IC emission is negligible because of the Klein-Nishina suppression.

Figure 1 indicates that all protons above 10^{15} eV may lose their energies for $R = 10^{13}$ cm. The result of the numerical simulation shown in Figure 2 is consistent with the above discussion. Nucleons with energies $> 10^{15}$ eV are extinguished. The energy protons lose is mainly transferred to pions and synchrotron photons (see Table 1). The highest energy protons ($> 6 \times 10^{19}$ eV) cool via synchrotron radiation, so that the pion distribution has a break at $\sim 10^{19}$ eV. The low-energy tail of the synchrotron spectrum exhibits $n(\epsilon_\gamma) \propto \epsilon_\gamma^{-1.5}$, as is usually seen in the fast cooling case (Granot et al. 2000). The weak peak at $\sim 10^5$ eV in the synchrotron spectrum may be due to low-energy protons whose photopion “optical depth” is small enough. The IC spectrum is complex because of the Klein-Nishina suppression.

Even for $R = 10^{13.5}$ cm (Fig. 3), nucleons $> 10^{16}$ eV are depleted by 2 orders of

magnitude. Figure 4 shows the case for $R = 10^{14}$ cm. In this case GRBs can be sources of UHECRs, although nucleons $> 10^{20.5}$ eV are reduced by the synchrotron cooling. The maximum value of τ_π is ~ 1 because of the low photon density. The highest energy protons create a few pions and lose a few tens of percent of their energies.

3.2. Neutrinos

Using the same method, we simulate behavior of charged pions and muons until they decay into positrons (electrons) and neutrinos. The life times of pions and muons, $T_\pi = \gamma_\pi T_{\pi,0}$ and $T_\mu = \gamma_\mu T_{\mu,0}$, ($T_{\pi,0} = 2.6 \times 10^{-8}$ s and $T_{\mu,0} = 2.2 \times 10^{-6}$ s are the life times of pions and muons at rest, respectively) are independent of the shell width l . Therefore, the energies charged pions and muons lose before their decays depend on l differently from the proton cooling.

When a pion decays $\pi^+(\pi^-) \rightarrow \mu^+\nu_\mu(\mu^-\bar{\nu}_\mu)$, the energy fraction a muon obtains is $\sim m_\mu/m_\pi \sim 0.76$. The rest of the energy goes to a neutrino. We assume that the energy of a muon at its decay will be shared equally by a positron (electron), a neutrino, and an anti-neutrino. We neglect neutrinos due to neutron decay $n \rightarrow pe^-\bar{\nu}_e$, whose time-scale is much longer than t_d .

Figure 5 shows the resulting spectra of neutrinos and photons emitted by pions and muons for $R = 10^{13}$ cm and $l = 10^{10}$ cm. Pions and muons above the energy where the life time is comparable to the cooling time t_γ or dynamical time t_d (Waxman and Bahcall 1997; AT03) lose their energy before their decay. For $R = 10^{13}$ cm and $l = 10^{10}$ cm, one half of the initial energy of the pions is expended via synchrotron radiation, and muons also lose their energy via synchrotron ($\sim 35\%$) and IC ($\sim 17\%$) radiation. Neutrinos are distributed as $n_\nu(\epsilon_\nu) \propto \epsilon_\nu^{-2}$ with a low- and high-energy cut-off.

The high-energy cut-off is determined by the life-time and the cooling time of pions (muons). Since a larger l leads to a lower U_B , the high-energy cut-off is roughly proportional to $l^{0.5}$ (see Fig. 6). Wider shell decreases the contribution of IC photons in comparison with synchrotron radiation, because of the Klein-Nishina suppression.

The low-energy cut-off is determined by the minimum energy of pions produced from protons, which depends on only R , as was discussed in §3.1. Both the low-energy and high-energy cut-off increase roughly $\propto R$ (see Fig. 7). If we observe neutrinos from GRBs, the spectra give us parameters such as l and R independently of gamma-ray observation.

Figure 8 shows the ratio of the neutrino energy to the initial proton energy ($\geq 10^{10}$ eV

at injection). For $R \leq 10^{14}$ cm, $\sim 10\%$ of the proton energy will be converted to a neutrino burst. If we consider only muon neutrinos, which will be detected with a kilometer-scale detector, their energy fraction may be a few percent of the accelerated protons. This result is consistent with the prediction of Dermer and Atoyan (2003).

The neutrino energy is a part of the energy protons lose via photopion production and synchrotron radiation. The “rest energy” (the energies of neutral pions, photons, electrons, and positrons) will be converted to lower energy photons ($< 10^9$ eV) via electromagnetic cascades (see AT03), because higher energy photons ($> 10^9$ eV) will be absorbed by electron-positron pair creation. The total energy of such photons is quite larger than the neutrino energy (see Fig. 9). If the energy of Fermi-accelerated protons above 3×10^{19} eV is comparable to the GRB photon energy E_γ , the energy of protons $> 10^{10}$ eV is $4.5E_\gamma$. Thus, the energy of protons may be 1-5 E_γ . In any case the energy of nucleons above 3×10^{19} eV will be lost for $R < 10^{14}$ cm. As long as the energy of UHECRs is assumed to be comparable to the GRB energy, gamma-ray photons originating from protons may be a large contribution to the GRB photons.

4. CONCLUSIONS AND DISCUSSION

Our simulations have shown that internal shocks should occur at radii $\geq 10^{14}$ cm to generate UHECRs, although significant GRB pulses have shorter time-scales of < 1 s (Norris et al. 1996). On the other hand, neutrino bursts are expected for $R < 10^{14}$ cm, while ultra-high-energy protons are depleted. The energy fraction of the neutrinos and neutrino spectra have been calculated for various R and l . Neutrino spectra give us information on the physical condition of GRBs, although only the most powerful bursts, which are brighter than 10^{53} erg or occur at $z < \sim 0.1$, produce detectable neutrino bursts with a kilometer-scale detector (Dermer and Atoyan 2003).

Smaller E_γ and larger R are favorable to generate UHECRs. At $R = 10^{14}$ cm, the most probable shell width is $l \sim R/\Gamma \sim 10^{12}$ cm. In this case the magnetic field becomes 8×10^3 G assuming $E_\gamma = 10^{51}$ ergs and $U_B = 0.1U_\gamma$. This strength seems rather weak to produce observed gamma-ray photons. Since there are some unsolved problems and ambiguous points in the theory of GRB spectra (Preece et al. 1998; Totani 1999; Asano and Kobayashi 2003), we have simply adopted a typical observed spectra without considering any physical conditions. It is challenging to find a condition to make both UHECRs and typical gamma-ray spectra be consistent.

To produce both UHECRs and a neutrino burst at the same time, the radius is limited

to around $R \sim 10^{14}$ cm in our case. Throughout this paper, we have adopted a relatively small GRB energy $E_\gamma = 10^{51}$ ergs as an optimistic case. For brighter bursts ($E_\gamma > 10^{51}$ ergs), stronger magnetic fields ($U_B \sim U_\gamma$), and smaller Lorentz factors ($\Gamma < 300$), internal shocks should occur at more distant radii to generate UHECRs. The threshold radius behaves as roughly $\propto E_\gamma^{1/2} \Gamma^{-1/2}$ under our assumption.

If protons are accelerated to very high energies at both the internal shock phase and afterglow phase, both UHECRs and neutrino burst may be produced. In this case the neutrino bursts may be originated from internal shocks, while most of the UHECRs are produced at the afterglow phase.

Throughout this paper the internal shock model has been applied. However, the external shock model may be applicable for smooth profile GRBs. According to Dermer (2002), the neutrino flux from individual GRBs is far too weak in the external shock model, while neutrino bursts occur in the internal shock model as shown in this paper. In the external shock model, ultra-high-energy neutrons are produced and travel ~ 100 kpc before their numbers are depleted by β -decay. Therefore, the external shock model predicts detection of neutron β -decay halo emission at optical and radio frequencies with luminosity $\sim 10^{35}$ ergs s $^{-1}$. On the other hand UHECRs may be extinguished for bright GRBs in the internal shock model so that neutron β -decay halos are not generated. Future neutrino, optical, and radio observations may provide tests of the two scenarios. Measurement of ion composition of UHECRs from supernova remnants with instruments such as *Auger* may be helpful for investigating the origin of UHECRs.

Neutrino bursts surely accompany gamma-ray photons originating from pion cascades. Those photons may be not negligible in comparison with the “original GRB photons.” In this case, as AT03 discussed, GRB photons may arise from pion cascades, rather than from initially existing electrons.

The author thanks the referee for useful comments.

REFERENCES

- Asano, K., & Kobayashi, S. 2003, PASJ, 55, 579
- Asano, K., & Takahara, F. 2003, PASJ, 55, 433 (AT03)
- Dermer, C. D. 2002, ApJ, 574, 65
- Dermer, C. D., & Atoyan, A. 2003, Phys. Rev. Lett., 91, 071102
- Frail, D. A., Kulkarni, S. R., Sari, R., Djorgovski, S. G., Bloom, J. S., Galama, T. J., Reichart, D. E., Berger, E., Harrison, F. A., Price, P. A., Yost, S. A., Diercks, A., Goodrich, R. W., & Chaffee, F. 2001, ApJ, 562, L55
- Granot, J., Piran, T., & Sari, R. 2000, ApJ, 534, L163
- Guetta, D., Hooper, D., Alvarez-Muñiz, J., Halzen, F., & Reuveni, E. 2004, Astroparticle Phys., 20, 429
- Guetta, D., Spada, M., & Waxman, E. 2001b, ApJ, 559, 101
- Mitrofanov, I. G., Pozanenko, A. S., Briggs, M. S., Paciesas, W. S., Preece, R. D., Pendleton, G. N., & Meegan, C. A. 1998, ApJ, 504, 925
- Norris, J. P., Nemiroff, R. J., Bonnell, J. T., Scargle, J. D., Kouveliotou, C., Paciesas, W. S., Meegan, C. A., & Fishman, G. J. 1996, ApJ, 459, 393
- Piran, T. 1999, Phys. Rep., 314, 575
- Preece, R. D., Briggs, M. S., Mallozzi, R. S., Pendleton, G. N., Paciesas, W. S., & Band, D. L. 1998, ApJ, 506, L23
- Rachen, J. P., & Mészáros, P. 1998, Phys. Rev. D, 58, 123005
- Rybicki, G. B., & Lightman, A. P. 1979, Radiative Processes in Astrophysics (New York: Wiley-Interscience)
- Stecker, F. W. 1968, Phys. Rev. Lett., 21, 1016
- Stecker, F. W. 1973, Ap&SS, 20, 47
- Totani, T. 1999, MNRAS, 307, L41
- Waxman, E. 1995, Phys. Rev. Lett., 75, 386

Waxman, E., & Bahcall, J. 1997, Phys. Rev. Lett., 78, 2292

Waxman, E., & Bahcall, J. 1999, Phys. Rev. D, 59, 023002

Wick, S. D., Dermer, C. D., & Atoyan, A. 2004, Astroparticle Phys., 21, 125

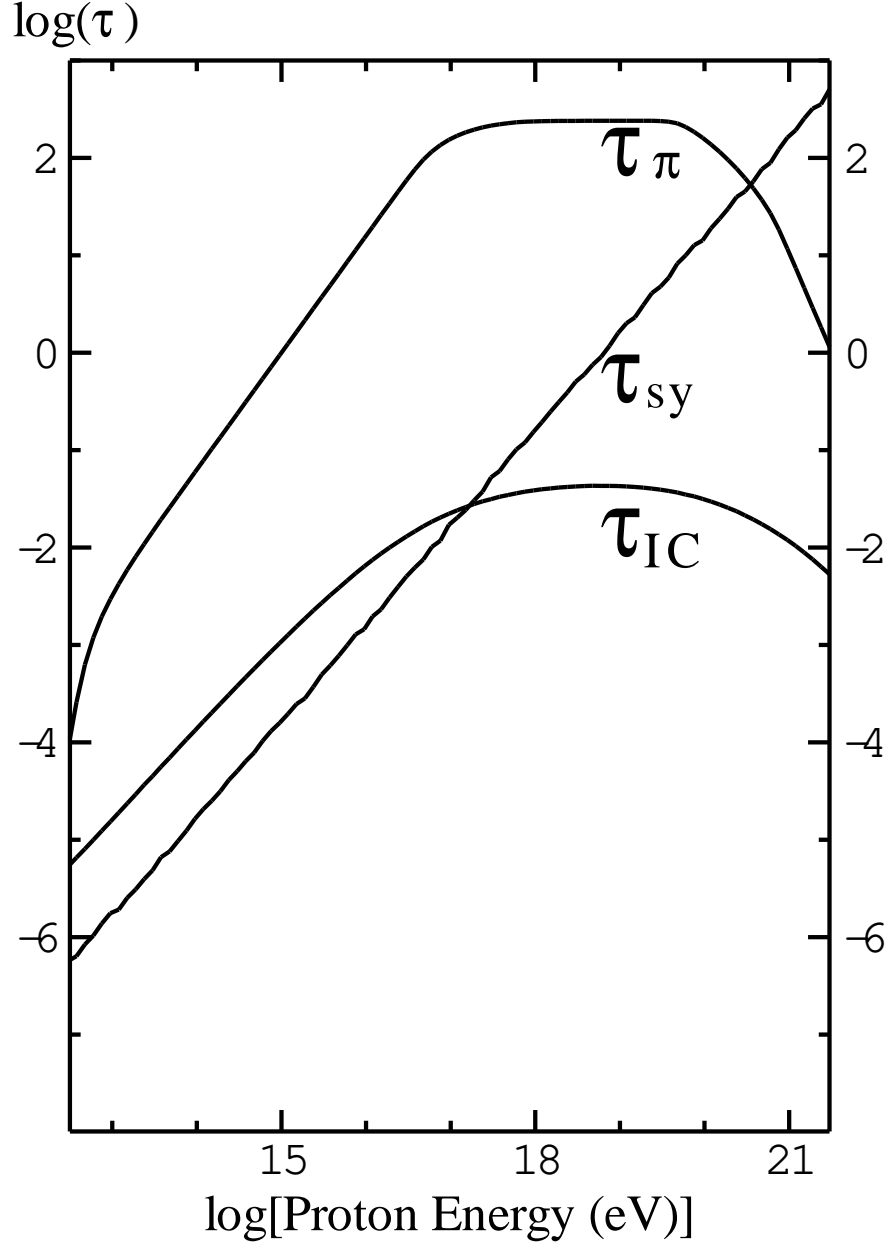


Fig. 1.— Proton cooling efficiencies $\tau_\pi, \tau_{\text{SY}}, \tau_{\text{IC}}$ for $R = 10^{13}$ cm and $E_\gamma = 10^{51}$ ergs. The proton energies are measured in the observer frame.

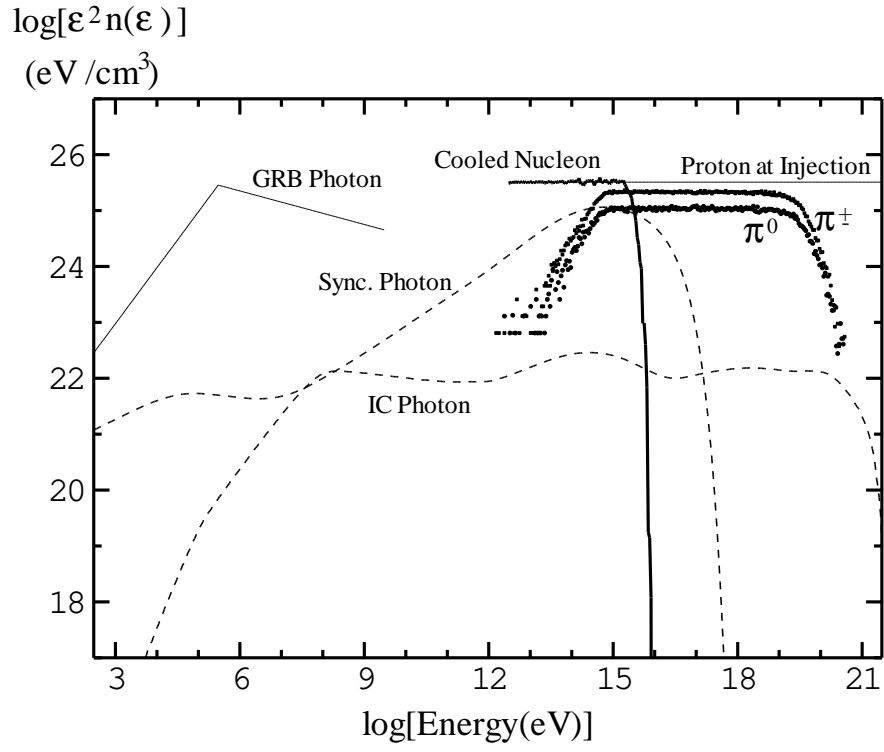


Fig. 2.— Spectra of GRB photons, protons at injection, created pions, photons emitted by protons (*dashed lines*), and cooled nucleons (protons and neutrons) for $R = 10^{13}$ cm.

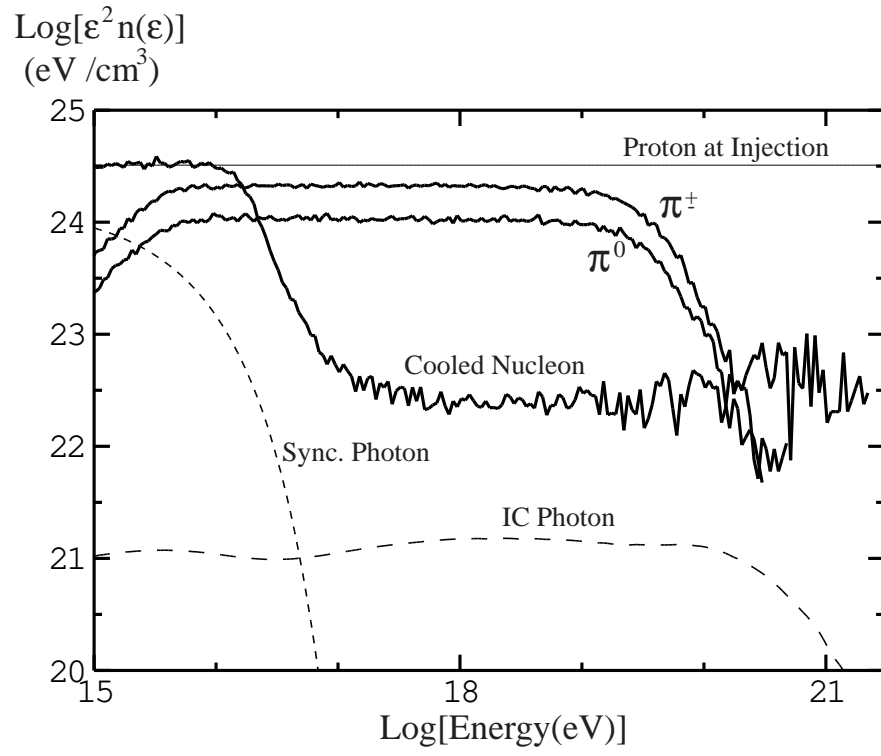


Fig. 3.— Same as Fig. 2, but for $R = 10^{13.5}$ cm.

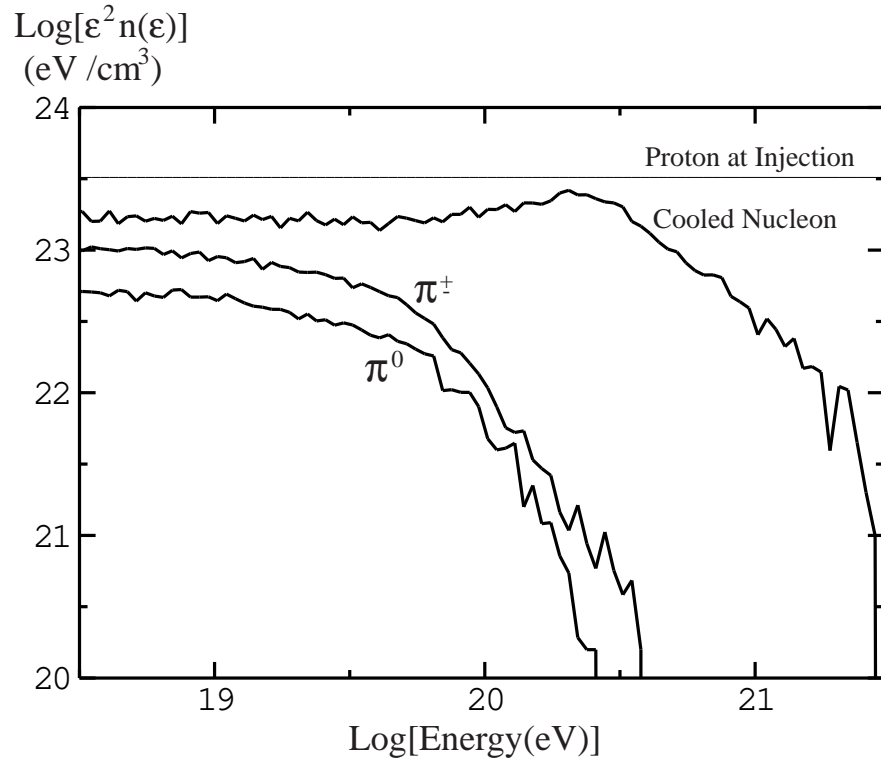


Fig. 4.— Same as Fig. 2, but for $R = 10^{14}$ cm.

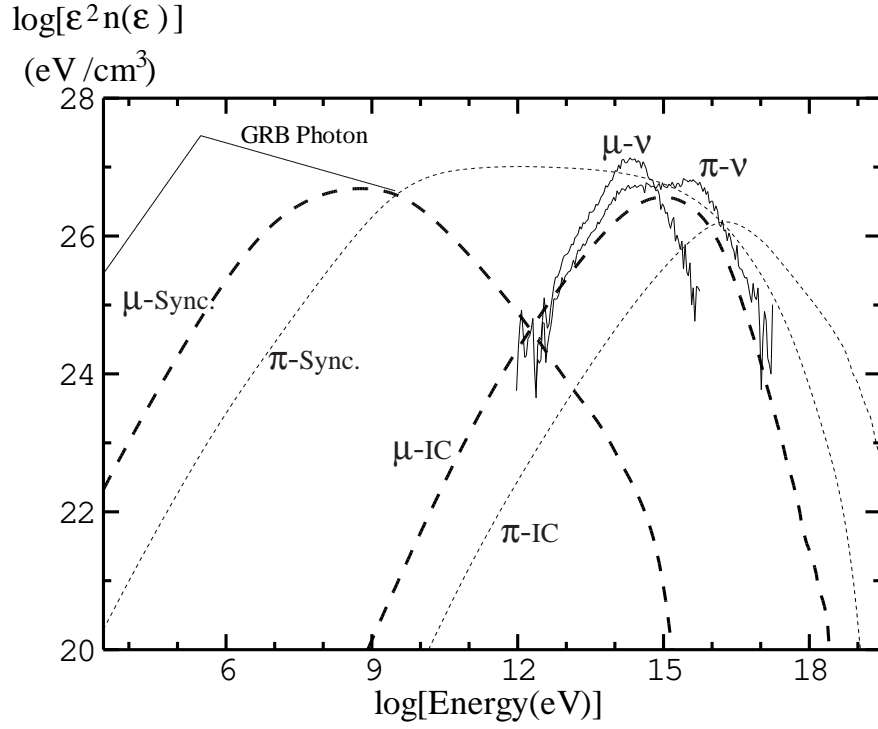


Fig. 5.— Spectra of neutrinos (*solid lines*) from pion decay (ν_μ and $\bar{\nu}_\mu$) and muon decay (ν_e , $\bar{\nu}_e$, ν_μ and $\bar{\nu}_\mu$) and synchrotron and IC photons emitted by pions (*thin dashed lines*) and muons (*thick dashed lines*) for $R = 10^{13}$ cm and $l = 10^{10}$ cm.

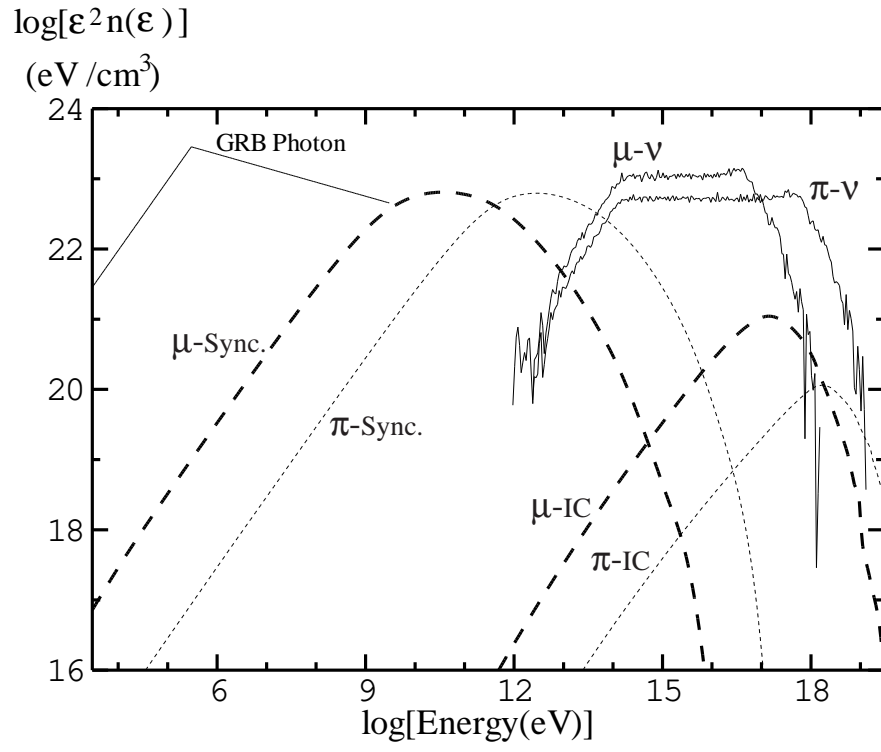


Fig. 6.— Same as Fig. 5, but for $l = 10^{14}$ cm.

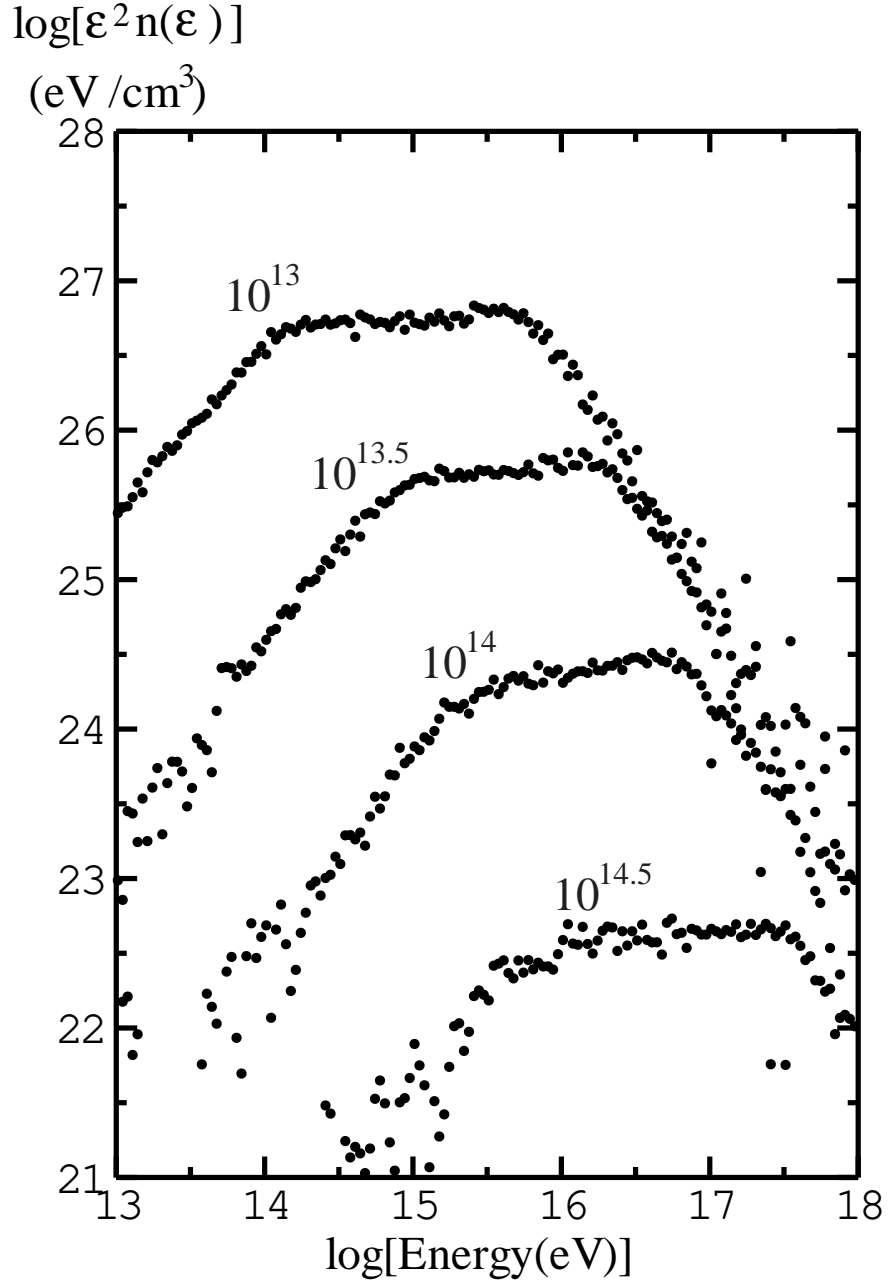


Fig. 7.— Spectra of neutrinos from pion decay for $l = 10^{10}$ cm. The radius R changes from 10^{13} to $10^{14.5}$ cm.

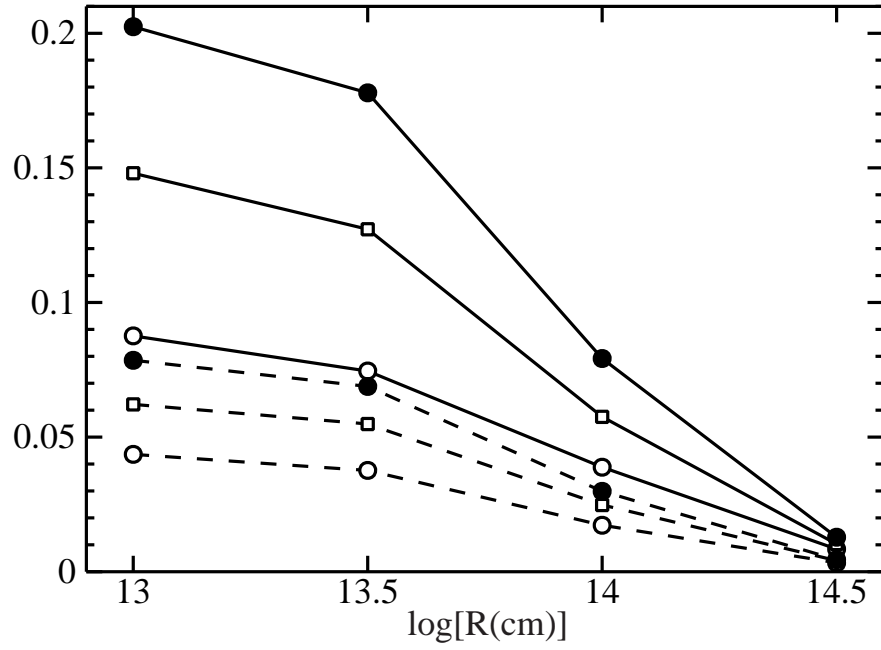


Fig. 8.— Ratio of neutrino energy to the initial proton energy. Dashed lines are for neutrinos originated from pions only, and solid lines are the total fraction. The shell width is assumed to be 10^{10} (*open circles*), 10^{12} (*rectangles*), and 10^{14} (*filled circles*) cm, respectively.

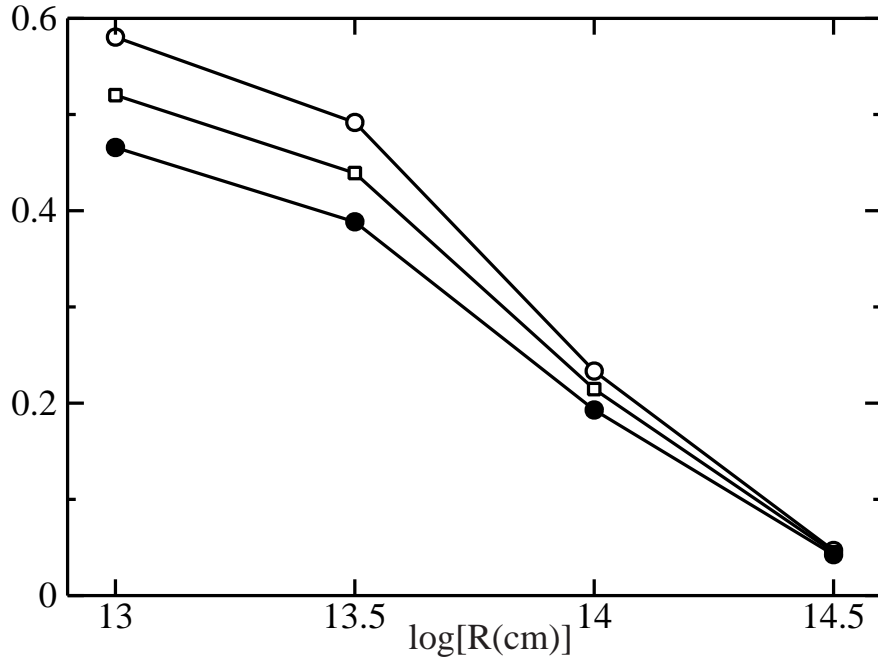


Fig. 9.— Ratio of “rest energy” (see text), which will be converted to gamma-ray photons, to the initial proton energy. The shell width is assumed to be 10^{10} (*open circles*), 10^{12} (*rectangles*), and 10^{14} (*filled circles*) cm, respectively.

Table 1: Energy Fraction Each Species of Particle Contributes to the Total Energy of Protons at Injection.

R (cm)	N	π	γ
10^{13}	0.33	0.57	0.10
$10^{13.5}$	0.43	0.47	0.10
10^{14}	0.73	0.19	0.08
$10^{14.5}$	0.94	0.03	0.03
10^{15}	0.99	0.002	0.01

Note. — The notations N , π , and γ represent cooled nucleons, created π^0 and π^\pm , and photons emitted directly by protons, respectively.